Dyes and Pigments 99 (2013) 537–542

Contents lists available at SciVerse ScienceDirect

Dyes and Pigments

journal homepage: www.elsevier.com/locate/dyepig

A two-photon fluorescent probe for imaging hydrogen sulfide in living cells

Tianyu Liu [a,b], Xinfu Zhang [a], Qinglong Qiao [a], Chunyan Zou [a], Lei Feng [a], Jingnan Cui [a,*], Zhaochao Xu [a,b,**]

[a] State Key Laboratory of Fine Chemicals, Dalian University of Technology, Dalian 116012, China
[b] Dalian Institute of Chemical Physics, Chinese Academy of Sciences, Dalian 116023, China

ARTICLE INFO

Article history:
Received 17 May 2013
Received in revised form
22 June 2013
Accepted 25 June 2013
Available online 10 July 2013

Keywords:
Two-photon fluorescence microscopy
Fluorescent probes
Hydrogen sulfide
Thiolysis
High selectivity
Cells imaging

ABSTRACT

Fluorescent probes for hydrogen sulfide have received considerable attention because of the biological significance of H_2S recognized recently. Two-photo microscopy offers advantages of increased penetration depth, localized excitation, and prolonged observation time. However, two-photon fluorescent probes for H_2S are still rare. In this work, we introduced a dinitrophenyl ether group into the 4-position of 1,8-naphthalimide, which acts as the H_2S reactive site, to efficiently yield compound **NI**–**NHS** as a two-photo fluorescent probe for H_2S. The probe **NI**–**NHS** has a high selectivity for H_2S over competitive anions and sulfide-containing analytes. This probe exhibits turn-on fluorescence detection of H_2S in bovine serum and two-photon fluorescent imaging of H_2S in living cells.

1. Introduction

Hydrogen sulfide (H_2S) is well known for its unpleasant odor of rotten eggs. Just recently, H_2S is recognized as the third most important gasotransmitter for regulating cardiovascular, neuronal, immune, endocrine and gastrointestinal systems, along with nitric oxide and carbon monoxide [1–3]. Altered levels of H_2S have been linked to many diseases, such as Alzheimer's disease, Down's syndrome, diabetes and liver cirrhosis [4–6]. The endogenous levels of H_2S are achieved by enzymes such as cystathionine-β-synthase (CBS) in the brain and cystathionine-γ-lyase (CSE) in the liver and vascular and nonvascular smooth muscle [7,8]. Some reports showed that mitochondrial sulfide quinone oxidoreductase (SQR) and persulfide dioxygenase (ETHE1) are involved in the consumption of H_2S [9]. These findings in living systems would be very important and helpful to elucidate the biological roles of H_2S.

For the detection of H_2S, a variety of fluorescent probes have been developed [10–14], featured with high sensitivity, high spatial and temporal resolution [15–18]. These fluorescent probes for H_2S are based on specific chemical reactions by taking advantage of the reducing or nucleophilic properties of H_2S. In accordance with the fluorophores, the reported probes are mainly derived from rhodamine [19], fluorescein [20], dansyl [21], BODIPY [22], naphthalimide [23], resorufamine [24], NBD, [25], BMF, [26], coumarin [27,28], cresyl violet [29], genetically encoded fluorescent protein [30], pyrene [31], DCDHF [32], DCMC [33] and phenanthroimidazole [34]. By attaching a sub-cellular targetable group, fluorescent probes can image H_2S in specific regions of cells, like mitochondria [35] and lysosomes [36]. However, these fluorescent probes work with one photo microscopy (OPM) that requires short excitation wavelength, which has the disadvantages such as photobleaching, photo-damage, shallow penetration depth, and cellular auto-fluorescence. Two-photo microscopy (TPM), a new technique that utilizes two photos of lower energy for excitation, has become a vital tool in biology. Compared to traditional fluorescence microscopy, TPM offers intrinsic 3D resolution combined with reduced phototoxicity, increased specimen penetration, and negligible background fluorescence [37–40]. Unfortunately, two-photon fluorescent probes for H_2S are still rare [26,41].

In this work, we introduced dinitrophenyl ether group into 4 position of 1,8-naphthalimide, which acted as the H_2S reactive site [42], and easily obtained the two-photo fluorescent probe **NI**–**NHS**

* Corresponding author.
** Corresponding author. State Key Laboratory of Fine Chemicals, Dalian University of Technology, Dalian 116012, China.
E-mail addresses: jncui@dlut.edu.cn (J. Cui), zcxu@dicp.ac.cn (Z. Xu).

0143-7208/$ – see front matter © 2013 Elsevier Ltd. All rights reserved.
http://dx.doi.org/10.1016/j.dyepig.2013.06.031

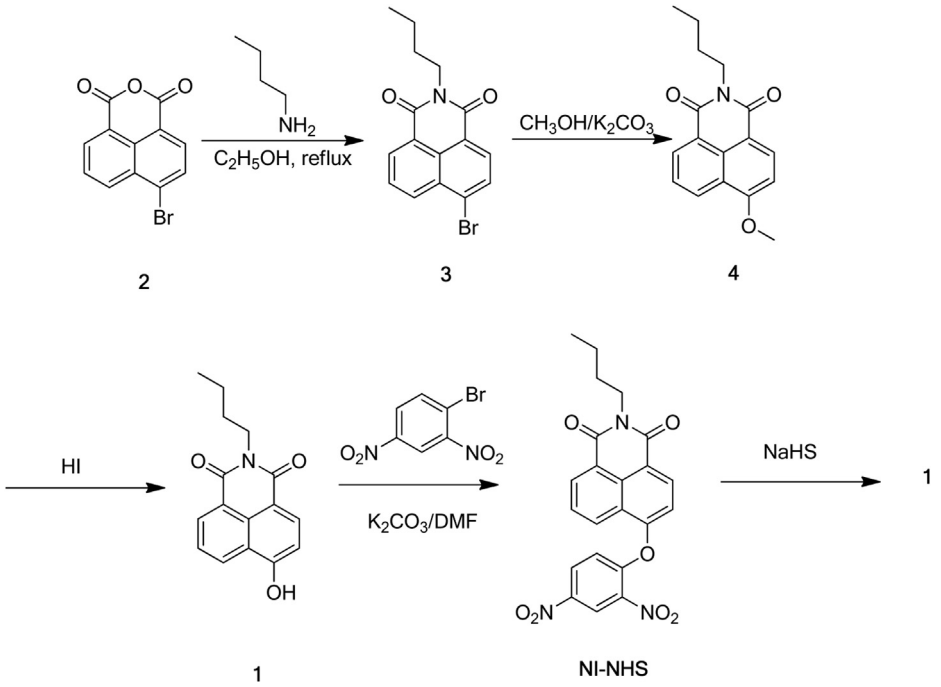

Scheme 1. Synthesis of the fluorescent probe **NI**–**NHS**.

[36]. The synthesis of **NI**–**NHS** is shown in Scheme 1, which is quite straightforward started from the cheap commercial available material 4-bromo-1,8-naphthalic anhydride. The probe **NI**–**NHS** was finally obtained in good yield and characterized by ^{1}H NMR, ^{13}C NMR and HRMS. The experimental details are given in supporting materials.

2. Experimental

2.1. Materials and instruments

Unless otherwise stated, all reagents were purchased from commercial suppliers and used without further purification.^{1}H NMR and ^{13}C NMR spectra were recorded on a VARIAN INOVA-400 spectrometer, using TMS as an internal standard. Mass spectrometry data were obtained with a HP1100LC/MSD mass spectrometer and an LC/Q-TOF MS spectrometer. UV–visible spectra were collected on a Perkin Elmer Lambda 35 UV/VIS spectrophotometer. Fluorescence measurements were performed on a VAEIAN CARY Eclipse fluorescence spectrophotometer (Serial No. FL0812-M018).

2.2. Synthesis

2.2.1. Synthesis of 4-bromo-N-butyl-1,8-naphthalimide (*3*)

4-bromo-1,8-naphthalic anhydride (**2**) (5 g, 0.018 mol) and n-butylamine (1.05 ml, 0.036 mol) were dissolved in 100 mL ethanol, and the solution was refluxed for 8 h. After cooling to room temperature, the yellowish sediments were collected by filtration and then dried overnight at room temperature in a vacuum oven to give **3** (5.5 g, yield: 91.7%). ^{1}HNMR (400 MHz, $CDCl_3$) δ 8.63 (d, $J = 7.3$ Hz, 1H), 8.53 (d, $J = 8.5$ Hz, 1H), 8.38 (d, $J = 7.9$ Hz, 1H), 8.01 (d, $J = 7.9$ Hz, 1H), 7.82 (t, 1H), 4.26–4.07 (m, 2H), 1.71 (m, 2H), 1.52–1.37 (m, 2H), 0.98 (t, 3H). HRMS (ESI) calcd for $C_{16}H_{14}BrNO_2$ [MH^+] 331.0208, found 331.0205.

2.2.2. Synthesis of N- butyl -4-methoxy-1,8-naphthalimide (*4*)

A mixture of compound **3** (1.66 g, 5 mmol) and K_2CO_3 (4.15 g, 25 mmol) in 30 mL CH_3OH was refluxed for 24 h. The precipitate was filtered and washed with water (30 mL × 3). Compound **4** was obtained as yellow needles (1.1 g, yield :78%). ^{1}H NMR (400 MHz, $CDCl_3$) δ 8.59 (d, $J = 7.3$, 1H), 8.55 (d, $J = 2.0$ Hz, 1H), 8.53 (d, $J = 2.1$ Hz, 1H), 7.69 (t, $J = 8.2$ Hz, 1H), 7.03 (d, $J = 8.3$ Hz, 1H), 4.20–

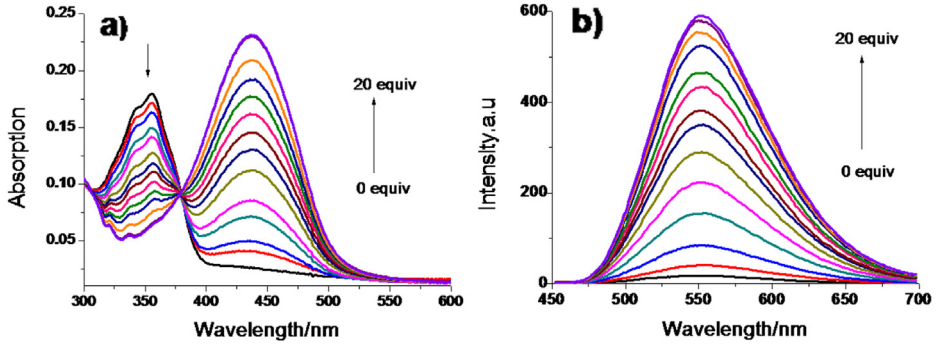

Fig. 1. a) UV–Vis absorption spectra of 10 μM compound **NI**–**NHS** in the presence of 0–20 equiv of H_2S in in aqueous solution (CH_3CN:PBS = 1:9, pH = 7.4, 37 °C) (NaHS was dissolved in water in the concentration of 10 mM). b) Corresponding fluorescent emission spectra respond to various H_2S concentrations. λ_{ex} = 450 nm.

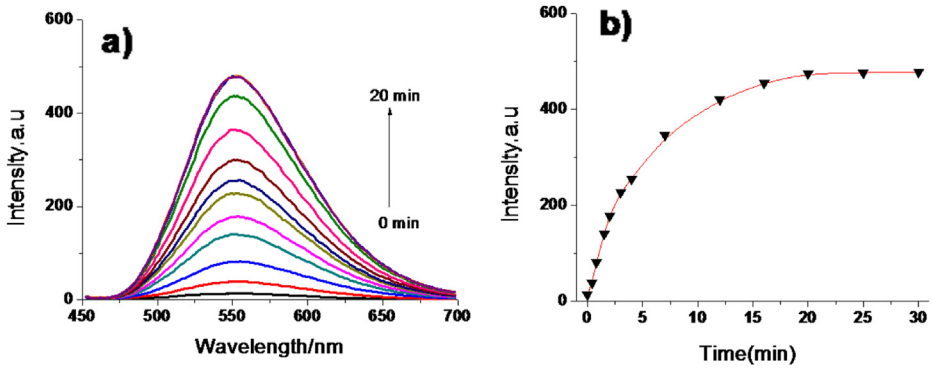

Fig. 2. a) Time dependence of fluorescence intensity of **NI**–**NHS** (10 μM) at 550 nm with 20 equiv H_2S (CH_3CN:PBS = 1:9, pH = 7.4, 37 °C). b) Time dependence of fluorescence profiles of **NI**–**NHS** (10 μM) with 20 equiv H_2S.

4.14 (m, 2H), 4.12 (s, 3H), 1.79–1.66 (m, 2H), 1.46 (m, 2H), 0.98 (t, 3H). HRMS (ESI) calcd for $C_{17}H_{17}NO_3$ [MH^+] 283.1208, found 283.1205.

2.2.3. Synthesis of N- butyl -4-hydroxy-1,8-naphthalimide (*1*)

A mixture of compound **4** (1 g, 3.5 mmol) and 50 mL concentrated HI (57%) was refluxed for 6 h. After cooling and adjusting pH to neutral, the precipitate was filtered to give compound **1** as yellow needles (0.81 g, yield :86.2%). ^{1}HNMR (400 MHz, DMSO) δ 11.85 (s, 1H), 8.50 (d, J = 8.3 Hz, 1H), 8.43 (d, J = 7.2 Hz, 1H), 8.33 (d, J = 8.2 Hz, 1H), 7.73 (t, J = 7.8 Hz, 1H), 7.14 (d, J = 8.2 Hz, 1H), 4.01 (t, J = 7.3 Hz, 2H), 2.53 (s, 1H), 1.68–1.52 (m, 2H), 1.42–1.25 (m, 2H), 0.93 (t, 3H). HRMS (ESI) calcd for $C_{16}H_{15}NO_3$ [MH^+] 269.1052, found 269.1051.

2.2.4. Synthesis of *NI*–*NHS*

Compound **1** (1 g, 3.7 mmol), 1-bromine-2,4-dinitrobenzene (1.5 g, 6.14 mmol) and K_2CO_3 (0.848 g, 6.14 mmol) were dissolved in anhydrous DMF (10 mL). The reaction mixture was then heated at 90 °C for 4 h under N_2 atmosphere. Cooling to room temperature, the reaction mixture was poured into ice water (100 mL). The crude product was extracted with ethyl acetate (3 × 25 mL) and dried over $MgSO_4$, and purified by flash column chromatography (ethyl acetate/CH_2Cl_2 = 1/1) to obtain the compound **NI**–**NHS** as a white solid (0.91 g, 56.2%). ^{1}HNMR (400 MHz, $CDCl_3$) δ 8.98 (d, J = 8.0, 1H), 8.71 (d, J = 8.0, 1H), 8.59 (d, J = 8.0 Hz, 1H), 8.48 (d, J = 8.4 Hz, 1H), 8.44 (d, J = 8.0 Hz, 1H), 7.85 (m, J = 8.4 Hz, 1H), 7.23 (m, 2H), 4.28–4.14 (m, 2H), 1.73 (m, 2H), 1.46 (m, 2H), 0.99 (t, 3H). ^{13}C NMR (100 MHz, $CDCl_3$) δ 163.80, 163.18, 155.30, 153.97, 143.2, 140.65, 132.48, 131.89, 129.88, 129.27, 127.96, 127.61, 124.20, 123.18, 122.45, 121.06, 120.39, 114.46, 40.40, 30.20, 20.38, 13.84. HRMS (ESI) calcd for $C_{22}H_{17}N_3O_7$ [MH^+] 435.1066, found 435.1069. Anal Calc for $C_{22}H_{17}N_3O_7$: C 60.66; H 3.94; N 9.64; O 25.72. Found C 60.62; H 3.95; N 9.66; O 25.73.

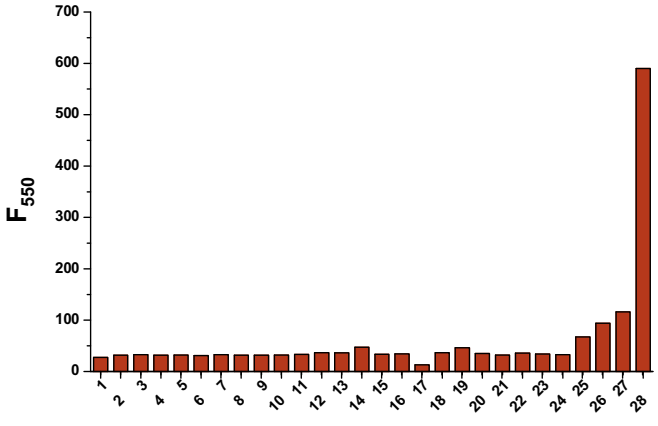

Fig. 3. Fluorescence responses of 10 μM **NI**–**NHS** to various analytes in aqueous solutions (CH_3CN:PBS = 1:9, pH = 7.4, 37 °C). λ_{ex} = 450 nm. Bars represent the final fluorescence intensity of **NI**–**NHS** with 1 mM analytes over the original emission of free **NI**–**NHS**. 1) free **NI**–**NHS**; 2) Na^+; 3) K^+; 4) Mg^{2+}; 5) Ca^{2+}; 6) Zn^{2+}; 7) F^-; 8) Cl^-; 9) Br^-; 10) I^-; 11) CO_3^{2-}; 12) H_2O_2; 13) SO_4^{2-}; 14)HCO_3^-; 15) NO_2^-; 16) CH_3COO^-; 17) HSO_4^-; 18) PO_4^{3-}; 19) CH_3COO^-; 20) N_3^-; 21) $S_2O_3^-$; 22) $S_2O_4^-$; 23) $S_2O_5^-$; 24) homocysteine; 25) ascorbic acid; 26) Cysteine; 27) Glutathione; 28) NaHS.

2.3. Culture of MCF-7 cells and fluorescent imaging

MCF-7(human breast carcinoma) was cultured in Dulbecco's modified Eagle's medium (DMEM, Invitrogen) supplemented with 10% FBS (fetal bovine serum) in an atmosphere of 5% CO_2 and 95% air at 37 °C. The cells were seeded in 24-well flat-bottomed plates and then incubated for 24 h at 37 °C under 5% CO_2. **NI**–**NHS** (5 μM) was then added to the cells and incubation for another 30 min followed. The cells were washed three times with phosphate-buffered saline (PBS). Fluorescence imaging was observed under a confocal microscopy (Olympus FV1000) with a 60 × objective lens.

3. Results and discussion

3.1. The spectroscopic properties of *NI*–*NHS* with H_2S in aqueous solutions

The absorption and fluorescence titration experiments of **NI**–**NHS** with H_2S were recorded in aqueous solution (CH_3CN:PBS = 1:9, pH = 7.4, 10 μM **NI**–**NHS**) (Fig. 1). In the absence of H_2S, **NI**–**NHS** presented a major absorption band at 358 nm. On addition of 0–20 equiv of H_2S to the solution of **NI**–**NHS**, the absorbance at 358 nm decreased sharply to its limiting value, while a new absorption band centered at 438 nm developed which induced the colour change from colourless to yellow (Fig. S1). The free **NI**–**NHS** displayed quite weak fluorescence. Importantly, with the addition of NaHS, the fluorescence intensity of **NI**–**NHS** increased significantly at 550 nm (37 fold) due to the thiolysis of the dinitrophenyl ether by H_2S. The MS and HPLC analysis confirmed that the fluorescence emission and enhancement was due to the formation of compound **1** (Fig. S2 and 3). The detection limit was calculated to be 0.18 μM (S/N = 3) (Fig. S4).

The influence of pH on the fluorescence of **NI**–**NHS** was determined by fluorescence titration (Fig. S5). The fluorescence at 550 nm of **NI**–**NHS** remains unaffected between pH 9-6.5, then gradually decreases from pH 6.5 to pH 3, and below pH 3 slight

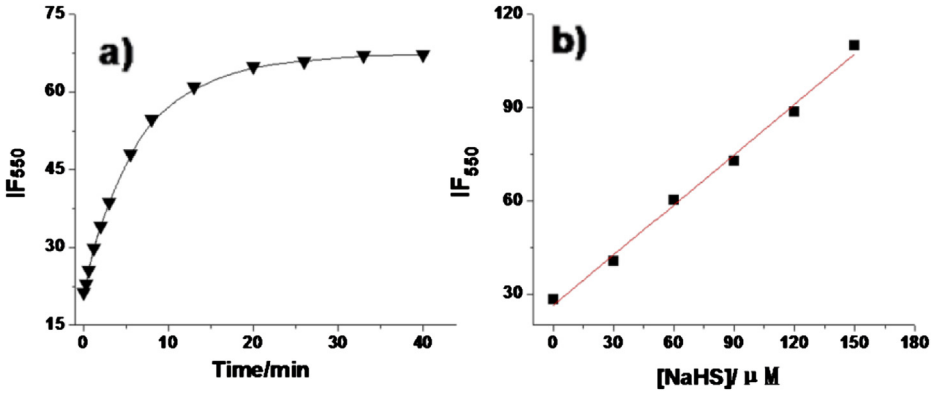

Fig. 4. (a) Fluorescence intensity of the probe **NI**–**NHS** (10 μM) incubated with 150 μM NaHS after 0 min, 0.3 min, 0.6 min, 1.2 min, 2 min, 3 min, 5.5 min, 8 min, 13 min, 20 min, 26 min, 33 min, 40 min in bovine serum at 25 °C. (b) **NI**–**NHS** probe (10 μM) incubated with 0, 30, 60, 90, 120, 150 μM NaHS after 20 min in bovine serum at 25 °C. The data represents the average of three independent experiments.

changes in fluorescence were finally obtained leading to a sigmoid curve. The studies of pH effect suggest that the compound **NI**–**NHS** is applicable in neutral medium like cells.

3.2. The time-dependent spectroscopic properties of *NI*–*NHS* with H_2S in aqueous solutions

The time-dependent fluorescence responses were next detected with the addition of 20 equiv H_2S and the results showed that the reaction was completed within 20 min (Fig. 2). Obviously, the background fluorescence of **NI**–**NHS** is very weak, and a high fluorescence increase is observed within several minutes which responses the reaction of **NI**–**NHS** with H_2S (Fig. 2b), then the timescale allows **NI**–**NHS** to sense H_2S in real-time intracellular imaging.

3.3. The selectivity of *NI*–*NHS* for H_2S

The probe **NI**–**NHS** (5 μM) was treated with various biologically relevant species to examine the selectivity. As shown in Fig. 3, **NI**–**NHS** showed selective response for H_2S over reactive oxygen species (ROS), reactive nitrogen species (RNS) and anions. Only ascorbic acid glutathione and cysteine gave limited increase in the fluorescence intensity. However, the intensity of the fluorescence increase was far weaker than that caused by H_2S. Thus, the probe **NI**–**NHS** has a very high selectivity for H_2S.

3.4. The spectroscopic properties of *NI*–*NHS* with H_2S in bovine serum

The tests in buffer solutions have shown the potential utility of **NI**–**NHS** in biological samples. We first checked the fluorescence response of **NI**–**NHS** with H_2S in bovine serum. The background fluorescence of bovine serum sample is relatively weak. With the addition of NaHS, the fluorescence intensity of emission of bovine serum sample with **NI**–**NHS** increases significantly. It should be noted that the fluorescence enhancement is observed immediately with the addition of NaHS and reaches the maximum value in minutes (Fig. 4a). The concentration-dependent fluorescence responses of **NI**–**NHS** with NaHS were next detected, and this produced a linear relationship of the fluorescence intensity of **NI**–**NHS** *versus* hydrogen sulphide concentration. As seen in Fig. 4b, an excellent linear correlation between the added NaHS concentration and the fluorescence intensity of **NI**–**NHS** at 550 nm was observed. The fast responses and excellent linear relationship provided a real-time quantitative detection method for hydrogen sulfide in biological samples.

3.5. Two-photon cell imaging of H_2S

We next tested the ability of **NI**–**NHS** to be used to visualize H_2S in live cells. OPM was first used. MCF-7 cells were incubated with **NI**–**NHS** (5 μM) for 30 min and exhibited no fluorescence (Fig. 5a). Then the cells were incubated with 50 μM NaHS, a concentration of H_2S comparable with physiological H_2S levels, and after 15 min displayed enhanced green fluorescence (Fig. 5b). We then tested the two-photon imaging ability of **NI**–**NHS** to detect H_2S in MCF-7 cells. Notably, the background fluorescence of **NI**–**NHS** is very weak without H_2S (Fig. 6a). Then the cells were incubated with 50 μM NaHS for 15 min. Upon TP excitation at 810 nm, the fluorescence intensity significantly increased (Fig. 6b). The cytotoxicity of **NI**–**NHS** was examined toward MCF-7 cells cells by an MTT assay (Figure S6). The results showed that ˃90% MCF-7 cells survived after 12 h (5.0 μM **NI**–**NHS** incubation), and after 24 h the cell viability

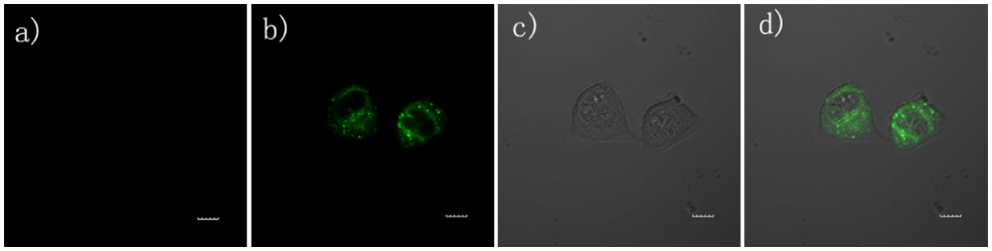

Fig. 5. Fluorescence imaging of H_2S in MCF-7 cells incubated with 5 μM **NI**–**NHS**. (a) **NI**–**NHS**; (b) **NI**–**NHS** with H_2S; (c) Bright field image; (d) Merged images of b) and c). Scale bars = 10 μm.

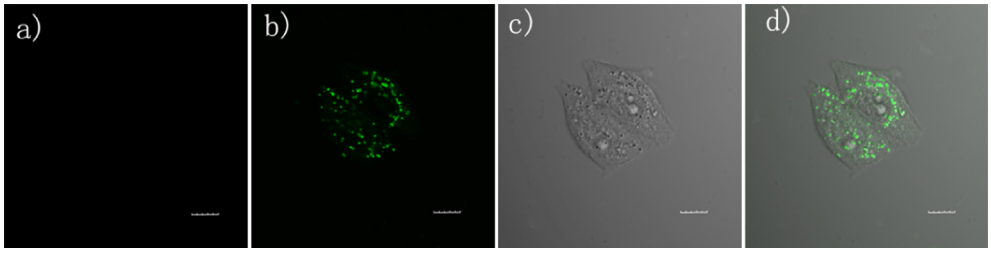

Fig. 6. TPM imaging of H_2S in MCF-7 cells incubated with 5 μM **NI**–**NHS**. (a) **NI**–**NHS**; (b) **NI**–**NHS** with H_2S; (c) Bright field image; (d) Merged images of b) and c). The two-photon excitation fluorescence was collected at 500–560 nm upon excitation at 810 nm. Scale bars = 10 μm.

remained at ~80%, demonstrating that **NI**–**NHS** was of low toxicity toward cultured cell lines. These experiments indicate that **NI**–**NHS** can act as a two-photo fluorescent probe to detect H_2S in living cells.

4. Conclusion

In summary, we developed a 1,8-naphthalimide-derived compound **NI**–**NHS** as a two-photo fluorescent probe for H_2S based on thiolysis of dinitrophenyl ether. Due to the rapid reaction of **NI**–**NHS** with H_2S, a large fluorescence increase was obtained with emission centered at 550 nm in aqueous solution. Concomitantly, the solution color changed from colourless to yellow. The probe displayed a high selectivity for H_2S over competitive reactive sulfur, oxygen, and nitrogen species. This probe is applicable to detect H_2S in bovine serum and living cells in TPM mode.

Acknowledgment

We thank financial support from the National Key Project for Basic Research of China (2009CB724706), Ministry of Human Resources and Social Security of PRC, the 100 talents program funded by Chinese Academy of Sciences, and State Key Laboratory of Fine Chemicals of China (KF1105).

Appendix A. Supplementary data

Supplementary data related to this article can be found at http://dx.doi.org/10.1016/j.dyepig.2013.06.031.

References

[1] Wang R. The gasotransmitter role of hydrogen sulfide. Antioxid Redox Sign 2004;5(4):493–501.
[2] Evans CL. The toxicity of hydrogen sulphide and other sulphides. Exp Physiol 1967;52(3):231–48.
[3] Kimura H. Hydrogen sulfide: its production, release and functions. Amino Acids 2011;41(1):113–21.
[4] Eto K, Asada T, Arima K, Makifuchi T, Kimura H. Brain hydrogen sulfide is severely decreased in Alzheimer's disease. Biochem Biophys Res Commun 2002;293(5):1485–8.
[5] Kamoun P, Belardinelli M-C, Chabli A, Lallouchi K, Chadefaux-Vekemans B. Endogenous hydrogen sulfide overproduction in down syndrome. Am J Med Genet A 2003;116A(3):310–1.
[6] Yang W, Yang G, Jia X, Wu L, Wang R. Activation of KATP channels by H2S in rat insulin-secreting cells and the underlying mechanisms. J Physiol 2005;569(2):519–31.
[7] Dominy JE, Stipanuk MH. New roles for cysteine and transsulfuration enzymes: production of H2S, a neuromodulator and smooth muscle relaxant. Nutr Rev 2004;62(9):348–53.
[8] Miller TW, Isenberg JS, Roberts DD. Molecular regulation of tumor angiogenesis and perfusion via redox signaling. Chem Rev 2009;109(7):3099–124.
[9] Hildebrandt TM, Grieshaber MK. Three enzymatic activities catalyze the oxidation of sulfide to thiosulfate in mammalian and invertebrate mitochondria. FEBS J 2008;275(13):3352–61.
[10] Xuan W, Sheng C, Cao Y, He W, Wang W. Fluorescent probes for the detection of hydrogen sulfide in biological systems. Angew Chem Int Ed 2012;51(10):2282–4.
[11] Peng H, Chen W, Burroughs S, Wang B. Recent advances in fluorescent probes for the detection of hydrogen sulfide. Curr Org Chem 2013;17(6):641–53.
[12] Lin VS, Chang CJ. Fluorescent probes for sensing and imaging biological hydrogen sulfide. Curr Opin Chem Biol 2012;16(5–6):595–601.
[13] Kumar N, Bhalla V, Kumar M. Recent developments of fluorescent probes for the detection of gasotransmitters (NO, CO and H2S). Coordination Chem Rev 2013;257(15–16):2335–47.
[14] Chan J, Dodani SC, Chang CJ. Reaction-based small-molecule fluorescent probes for chemoselective bioimaging. Nat Chem 2012;4(12):973–84.
[15] Xu Z, Zheng S, Yoon J, Spring DR. Discovery of a highly selective turn-on fluorescent probe for Ag+. Analyst 2010;135(10):2554–9.
[16] Guo Z, Song NR, Moon JH, Kim M, Jun EJ, Choi J, et al. A benzobisimidazolium-based fluorescent and colorimetric chemosensor for CO2. J Am Chem Soc 2012;134(43):17846–9.
[17] Xu Z, Liu X, Pan J, Spring DR. Coumarin-derived transformable fluorescent sensor for Zn2+. Chem Commun 2012;48(39):4764–6.
[18] Song NR, Moon JH, Choi J, Jun EJ, Kim Y, Kim S-J, et al. Cyclic benzobisimidazolium derivative for the selective fluorescent recognition of HSO4-via a combination of C–H hydrogen bonds and charge interactions. Chem Sci 2013;4(4):1765–71.
[19] Lippert AR, New EJ, Chang CJ. Reaction-based fluorescent probes for selective imaging of hydrogen sulfide in living cells. J Am Chem Soc 2011;133(26):10078–80.
[20] Liu C, Pan J, Li S, Zhao Y, Wu LY, Berkman CE, et al. Capture and visualization of hydrogen sulfide by a fluorescent probe. Angew Chem Int Ed 2011;50(44):10327–9.
[21] Peng H, Cheng Y, Dai C, King AL, Predmore BL, Lefer DJ, et al. A fluorescent probe for fast and quantitative detection of hydrogen sulfide in blood. Angew Chem Int Ed 2011;50(41):9672–5.
[22] Qian Y, Karpus J, Kabil O, Zhang S-Y, Zhu H-L, Banerjee R, et al. Selective fluorescent probes for live-cell monitoring of sulphide. Nat Commun 2011;2:495.
[23] Montoya LA, Pluth MD. Selective turn-on fluorescent probes for imaging hydrogen sulfide in living cells. Chem Commun 2012;48(39):4767–9.
[24] Chen B, Lv C, Tang X. Chemoselective reduction-based fluorescence probe for detection of hydrogen sulfide in living cells. Anal Bioanal Chem 2012;404(6–7):1919–23.
[25] Zhou G, Wang H, Ma Y, Chen X. An NBD fluorophore-based colorimetric and fluorescent chemosensor for hydrogen sulfide and its application for bioimaging. Tetrahedron 2013;69(2):867–70.
[26] Das SK, Lim CS, Yang SY, Han JH, Cho BR. A small molecule two-photon probe for hydrogen sulfide in live tissues. Chem Commun 2012;48(67):8395–7.
[27] Wu Z, Li Z, Yang L, Han J, Han S. Fluorogenic detection of hydrogen sulfide via reductive unmasking of o-azidomethylbenzoyl-coumarin conjugate. Chem Commun 2012;48(81):10120–2.
[28] Li W, Sun W, Yu X, Du L, Li M. Coumarin-based fluorescent probes for H2S detection. J Fluoresc 2013;23(1):181–6.
[29] Wan Q, Song Y, Li Z, Gao X, Ma H. In vivo monitoring of hydrogen sulfide using a cresyl violet-based ratiometric fluorescence probe. Chem Commun 2013;49(5):502–4.
[30] Chen S, Chen Z-j, Ren W, Ai H-w. Reaction-based genetically encoded fluorescent hydrogen sulfide sensors. J Am Chem Soc 2012;134(23):9589–92.
[31] Hartman MCT, Dcona MM. A new, highly water-soluble, fluorescent turn-on chemodosimeter for direct measurement of hydrogen sulfide in biological fluids. Analyst 2012;137(21):4910–2.
[32] Chen T, Zheng Y, Xu Z, Zhao M, Xu Y, Cui J. A red emission fluorescent probe for hydrogen sulfide and its application in living cells imaging. Tetrahedron Lett 2013;54(23):2980–2.
[33] Zheng Y, Zhao M, Qiao Q, Liu H, Lang H, Xu Z. A near-infrared fluorescent probe for hydrogen sulfide in living cells. Dyes Pigm 2013;98(3):367–71.
[34] Zheng K, Lin W, Tan L. A phenanthroimidazole-based fluorescent chemosensor for imaging hydrogen sulfide in living cells. Org Biomol Chem 2012;10(48):9683–8.
[35] Chen Y, Zhu C, Yang Z, Chen J, He Y, Jiao Y, et al. A ratiometric fluorescent probe for rapid detection of hydrogen sulfide in mitochondria. Angew Chem Int Ed 2013;52(6):1688–91.
[36] Liu T, Xu Z, Spring DR, Cui J. A lysosome-targetable fluorescent probe for imaging hydrogen sulfide in living cells. Org Lett 2013;15(9):2310–3.

[37] Helmchen F, Denk W. Deep tissue two-photon microscopy. Nat Methods 2005;2(12):932–40.
[38] Wang B, Wang Y, Hua J, Jiang Y, Huang J, Qian S, et al. Starburst triarylamine Donor–Acceptor–Donor quadrupolar derivatives based on cyano-substituted diphenylaminestyrylbenzene: tunable aggregation-induced emission colors and large two-photon absorption cross sections. Chem Eur J 2011;17(9):2647–55.
[39] Jiang Y, Wang Y, Hua J, Tang J, Li B, Qian S, et al. Multibranched triarylamine end-capped triazines with aggregation-induced emission and large two-photon absorption cross-sections. Chem Commun 2010;46(26):4689–91.
[40] Lu Z-J, Wang P-N, Zhang Y, Chen J-Y, Zhen S, Leng B, et al. Tracking of mercury ions in living cells with a fluorescent chemodosimeter under single- or two-photon excitation. Anal Chim Acta 2007;597(2):306–12.
[41] Sun W, Fan J, Hu C, Cao J, Zhang H, Xiong X, et al. A two-photon fluorescent probe with near-infrared emission for hydrogen sulfide imaging in bio-systems. Chem Commun 2013;49(37):3890–2.
[42] Cao X, Lin W, Zheng K, He L. A near-infrared fluorescent turn-on probe for fluorescence imaging of hydrogen sulfide in living cells based on thiolysis of dinitrophenyl ether. Chem Commun 2012;48(85):10529–31.